Applied Catalysis A: General 520 (2016) 1–6

Contents lists available at ScienceDirect

Applied Catalysis A: General

journal homepage: www.elsevier.com/locate/apcata

Photocatalytic and electrocatalytic reduction of CO_2 to methanol by the homogeneous pyridine-based systems

Wei Wang [a], Junxiao Zhang [b], Hui Wang [a,*], Lianjia Chen [a], Zhaoyong Bian [b,*]

[a] College of Environmental Science and Engineering, Beijing Forestry University, Beijing 100083, PR China
[b] College of Water Sciences, Beijing Normal University, Beijing 100875, PR China

ARTICLE INFO

Article history:
Received 7 January 2016
Received in revised form 23 March 2016
Accepted 5 April 2016
Available online 6 April 2016

Keywords:
Photocatalysis
CO_2 reduction
Methanol
Metal complex
Homogeneous catalysis

ABSTRACT

The visible light driven pyridine catalytic reduction of CO_2 was performed in aid of ruthenium phenanthroline complex photosensitizer. The light absorbance and utilization of the catalytic system was identified using UV–vis absorption and emission spectroscopic techniques. Under the dark conditions, electrochemical properties of the catalytic system were evaluated by compared the redox properties under N_2 and CO_2 pressure, respectively. Then, the photocatalytic CO_2 reduction with this catalytic system was studied under the visible light ($\lambda > 420$ nm) irradiation. The gaseous and liquid products of the CO_2 reduction were analyzed using gas chromatography and liquid chromatography. Methanol was the main product and there were no other products determined in the present system. The photocatalytic system showed a high product selectivity and efficient productivity with 60 μmol/L of methanol as solo product under the optimized conditions.

1. Introduction

The conversion of CO_2 to useful fuels powered by renewable energy has dramatically an effect in the energy and environmental fields. The attempts to fulfill the conversion are hot research spots and attract considerable attention [1–10]. The electrochemical reduction of CO_2 is one such process, which has been studied and produces alkanes, alcohols, and other desirable products under suitable reaction conditions [11]. However, this attractive technology for the production of carbon based chemicals suffered by the low selectivity, poorly defined reaction mechanisms, and large overpotentials which induced huge energy consumption [12]. Recently, the photocatalytic reduction of CO_2 is an attractive route that can take advantage of the renewable and abundant energy of the sun for long-term CO_2 utilization [13–21].

There are several ways to reduce CO_2 with the assistance of renewable solar energy, and these methods can be divided into two major categories: homogeneous photoreduction by a molecular catalyst and hetergeneous photoreduction by a semiconductor catalyst [14]. Semiconductors such as TiO_2 and SiC had been widely studied as heterogeneous catalysts for the photochemical conversion of CO_2 to a variety of carbon products such as carbon monoxide, methanol, and methane [15,22–24]. Nevertheless, examples of selective light-driven CO_2 conversion to reduced carbon products in heterogeneous systems were limited to the wide band gap, UV light responsible materials that do not exhibit high selectivity toward a single carbon product [25], aside from select transition-metal doped silicates [26–29]. Homogeneous molecular systems offer an alternative strategy for solar CO_2 fixation that allows for modular tuning of their performances via synthetic chemistry [16,30]. In aqueous systems, the pyridinium ion ($pyrH^+$) has been reported to act as a homogeneous catalyst for the electrochemical reduction of CO_2 with 30% Faradaic yields for methanol formation on hydrogenated palladium electrodes [31].

Photocatalytic reduction of CO_2 has become an interesting research topic because of the potential utilization of renewable solar energy [32–34]. Photochemical reductions of CO_2 with selective product formation using rhenium polypyridine catalysts had been extensively studied, however, rhenium complexes mainly absorb the UV light and could not utilize the full solar spectrum [35,36]. And the visible light photocatalytic CO_2 reduction system suffered from the noble-metal catalysts that achieve low turnover numbers and/or selectivity [16]. Related systems with $[Ru(bpy)_3]^{2+}$ as a photosensitizer and transition metal complexes have reported with rare yield of CO but concomitant H_2 production with a high yield [37–41]. Highly efficient and selective photocatalysts that could function under sunlight are important for solar hydrocarbon production [34,42]. It is urged to achieve sustainable, solar

* Corresponding author.
E-mail addresses: wanghui@bjfu.edu.cn (H. Wang), bian@bnu.edu.cn (Z. Bian).

http://dx.doi.org/10.1016/j.apcata.2016.04.003
0926-860X/

CO_2 conversion to a predominant product with high selectivity and activity.

In this article, a visible light driven CO_2 reduction with pyridine as catalyst was reported. To conform the efficiency of this system, electrochemical technologies such as cyclic voltammetry (CV) and differential pulse voltammetry (DPV) was used to investigate the redox properties of the pyridine catalyst and ruthenium complex photosensitizer. Absorption spectra of the system was studied to evaluate the light utilization. In a homemade photocatalytic reactor, the photocatalytic reduction of CO_2 was performed under the visible light irradiation. The solo determined product of the reduction was methanol.

2. Experimental

2.1. Synthesis of Ru complex

$[Ru(phen)_3](PF_6)_2$ was prepared with slight modifications to a literature method [43]. $RuCl_3$ (0.42 g, 2 mmol) and 1,10-phenanthroline (1.09 g, 6 mmol) were added in an ethanol solution and heated to reflux with stirring under an atmosphere of N_2 for 8 h. Then the solution was cooled down to room temperature. Subsequently NH_4PF_6 (3.26 g, 20 mmol) saturated solution was added to the solution to form a red precipitate. The solid was filtered and dried under vacuum overnight.

2.2. Analytical method

^1H NMR spectra was recorded at 25 °C at Bruker AV500 500 MHz Nuclear Magnetic Resonance spectrometer. The chemical shift was adjusted to zero with tetramethylsilane as a reference substance.

UV–vis absorption spectra was acquired on UV-2600 spectrometer (Shimadzu, Japan) using screw cap quartz cuvettes of 1 cm pathlength. All absorption spectra were recorded at room temperature and all samples were prepared in acetonitrile: water = 1:1. Concentration of the solution was 0.02 mmol/L and scan wavelength range was 200–800 nm.

The photoluminescence (PL) spectra was measured by the F-7000 (Hitachi, Japan) using screw cap quartz cuvettes of 1 cm pathlength. All absorption spectra were recorded at room temperature and all samples were prepared in acetonitrile: water = 1:1. Concentration of the solution was 0.02 mmol/L and scan wavelength range was 500–800 nm.

Electrochemical measurements of the complex are performed on a CHI660D electrochemical workstation (Chenhua, China) using a standard three-electrode cell with a platinum wire as working electrode, a standard Ag/AgCl in saturated KCl as reference electrode, and a platinum wire as counter electrode. Tetrabutylammonium hexafluorophosphate (0.1 mol/L) and potassium chloride (0.5 mol/L) were used as electrolyte reagents. CV measurement of pyridine (5.24 mmol/L) with different scanning speeds, pH and different electrolyte concentration were performed. Prior to measurement, the solutions were sparged with N_2 and CO_2 gas for 40 min, respectively.

2.3. Visible-light photoredox method for CO_2 reduction

$[Ru(phen)_3](PF_6)_2$ (0.020 mmol/L), pyridine (50 mmol/L), KCl (0.1 mmol/L) and ascorbic acid (0.2 mmol/L) were mixed in 25 mL of acetonitrile solution and added in a 50 mL glass tube reactor. The pH of solution was adjusted to 4, 5, and 6 respectively with hydrochloric acid and sodium hydroxide. The samples were charged with a stir bar and the system was sealed with a rubber septum which was tightened with a copper wire. The sample solution and reactor headspace was saturated with CO_2. The samples were irradiated by a 500 W Xe arc lamp. The wavelength of light was controlled by a long pass filter ($\lambda > 420$ nm) that was immersed in water. Light was focused onto the stirred sample and irradiated for 1–6 h. After irradiation, aliquots were analyzed by CP-3800 gas chromatography (Varian, USA) coupled with a flame ionization detector (GC-FID). The reaction apparatus is shown in Fig. 1.

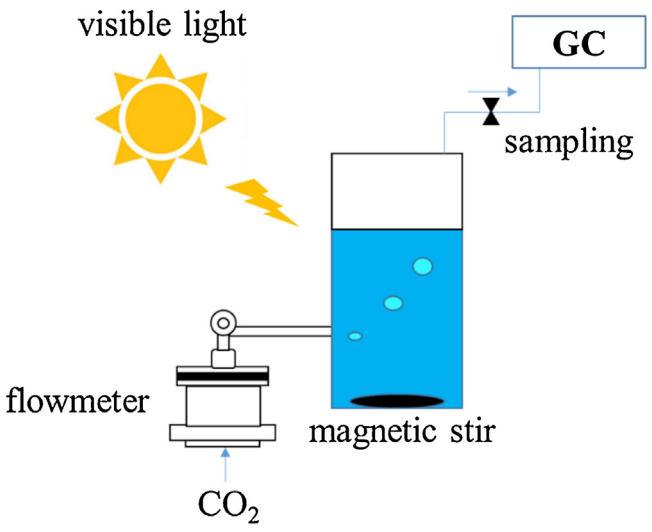

Fig. 1. Scheme of the photocatalytic reaction device.

3. Results and discussion

3.1. Synthesis and characterization of photosensitizer

NMR spectrum of $[Ru(phen)_3](PF_6)_2$ complex is shown in Fig. 2. ^1H NMR (500 MHz, $CDC1_3$): δ 8.76 (dd, 6H), 8.22 (dd, 6H), 7.92 (dd, 6H) which were in accord with refer data [44].

Absorption spectra and emission spectra of ruthenium complex photosensitizer are shown in Fig. 3.

As shown in the UV–vis absorption spectrum of ruthenium complex (Fig. 3(a)), the dominant feature in the visible region was a broad metal to ligand charge transfer (MLCT) absorption band centered at 451 nm that presume the complex had a certain of absorption and response in the visible region. In the UV region, the intense bands were assigned to the ligand-based π-π^* transition (^{1}IL) of phenanthroline ligand [45]. As shown in Fig. 3(b), the excited ruthenium complex photosensitizer gave a strong emission centered at 600 nm. CV and DPV of ruthenium complex are shown in Fig. 4.

As shown in Fig. 4(a), the first oxidation potential was occurred at 1.20 V corresponding to the peak of DPV at 1.20 V, which represented the oxidation potential of $[Ru^{II}(phen)]^{2+}$ losing one electron shown in Eq. (1). Subsequent, reduction potential occurred at −1.38 V, −1.64 V, −1.85 V corresponding to the peaks of DPV at −1.38 V, −1.64 V, −1.85 V, which can be speculated by the reduction process of Eqs. (2)–(4) [43].

$$[Ru^{II}(phen)_3]^{2+} - e^- \rightarrow [Ru^{III}(phen)_3]^{3+} E_{1/2} = 1.20\,V \quad (1)$$

$$[Ru^{II}(phen)_3]^{2+} + e^- \rightarrow [Ru^{II}(phen)_2(phen^-)]^{1+} E_{1/2} = -1.38\,V \quad (2)$$

$$[Ru^{II}(phen)_2(phen^-)]^{1+} + e^- \rightarrow [Ru^{II}(phen)(phen^-)_2]^{\bullet} E_{1/2} = -1.64\,V \quad (3)$$

$$[Ru^{II}(phen)(phen^-)_2]^{\bullet} + e^- \rightarrow [Ru^{II}(phen^-)_3]^- E_{1/2} = -1.85\,V \quad (4)$$

It indicated that $[Ru^{II}(phen^-)_3]^-$ was of vital importance for photoinduced electron transfer, which certified why the complex was good at photocatalysis.

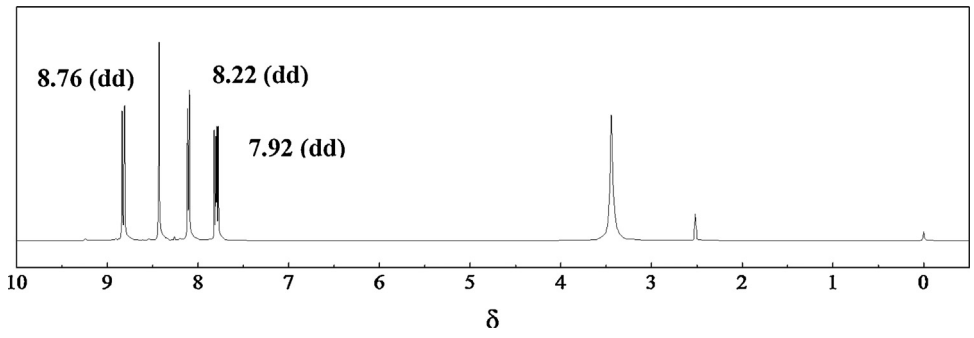

Fig. 2. NMR spectrum of $[Ru(phen)_3](PF_6)_2$ complexes.

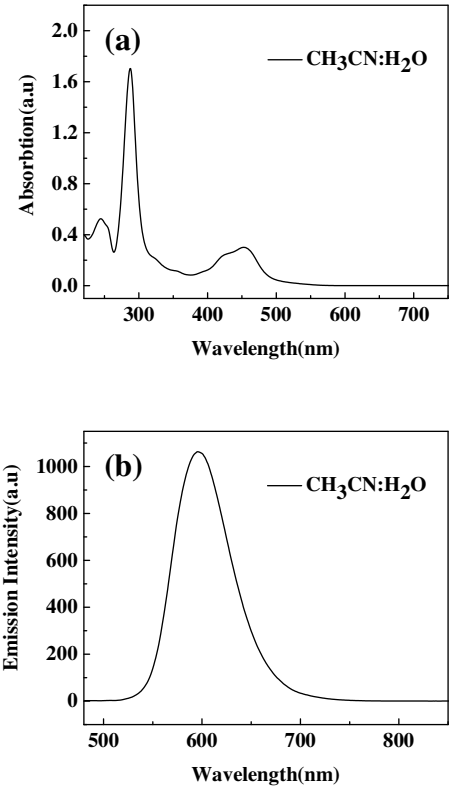

Fig. 3. UV-vis absorption spectrum (a) and emission spectrum of complexes (b) in $CH_3CN:H_2O$ (1:1) solutions.

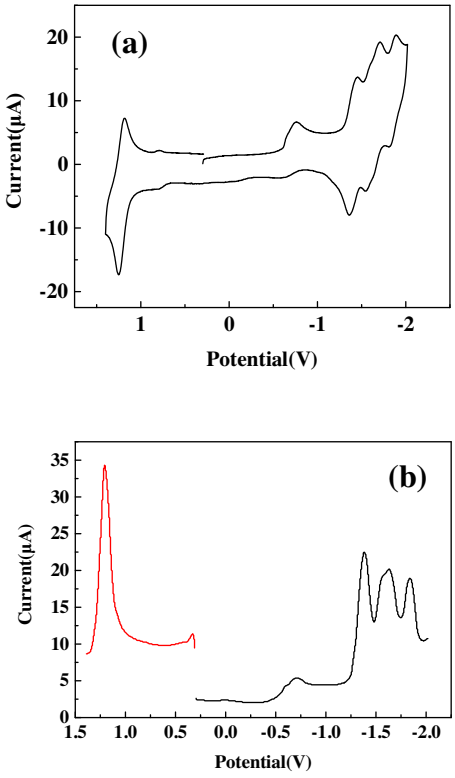

Fig. 4. CV (a) and DPV (b) of complexes with tetrabutylammonium hexafluorophosphate (0.1 mol/L) and $[Ru(phen)_3](PF_6)_2$ (5 mmol/L) in acetonitrile solution; scan rate, 100 mV/s; All potentials were in volts vs. the Fc^+/Fc couple.

In order to investigate the effect of the sacrificial agent on the photocatalytic reduction of CO_2, ascorbic acid was chosen respectively as a quencher to test fluorescence quenching experiment of ruthenium complex. The effect of different concentration of ascorbic acid in the quenching experiment is shown in Fig. 5.

As shown in Fig. 5(a), the emission intensity of the ruthenium complex photosensitizer decreased with the increase of the concentration of ascorbic acid as the quenching agent. Fig. 5(b) shows that relationship between emission peak intensity/initial intensity and concentration of ascorbic acid was linear with R^2, 0.9914 which proved that ascorbic acid was the appropriate sacrificial agent in experiment of photocatalytic reduction of CO_2. The results indicated that ascorbic acid could efficiently quench the excited ruthenium complex photosensitizer to form reduced species which could transfer electrons to the CO_2 reduction reaction.

3.2. Evaluation of pyridine for electrocatalytic CO_2 reduction

CV of pyridine is performed under N_2 and CO_2 pressure in Fig. 6.

As shown in Fig. 6, the reduction peak under CO_2 pressure was significantly greater than that under N_2, which proved that it occurred redox reaction between pyridine catalyst and CO_2. In these processes, pyridine was protonated to form pyridinium PyH^+. PyH^+ was reduced to form PyH^+ after accept an electron under the reduction potential. Then PyH^+ could react with CO_2 to form $PyCOOH^+$ in the homogeneous phase which becomes further reduced into CH_3OH through a series of subsequent reduction steps [42].

To investigate the rate determined step in these processes, CV spectra were repeated with different scanning speeds which are shown in Fig. 7.

As shown in Fig. 7(a), the reduction current became bigger with the increase of the scan rate. In order to study whether the electrode was affected by adsorption and diffusion controlled, peak current was plotted with scan speed and the square root of the scanning rate, respectively. Fig. 7(b) and (c) show that relationship between peak current and scan rate was linear with R^2, 0.9316 which were

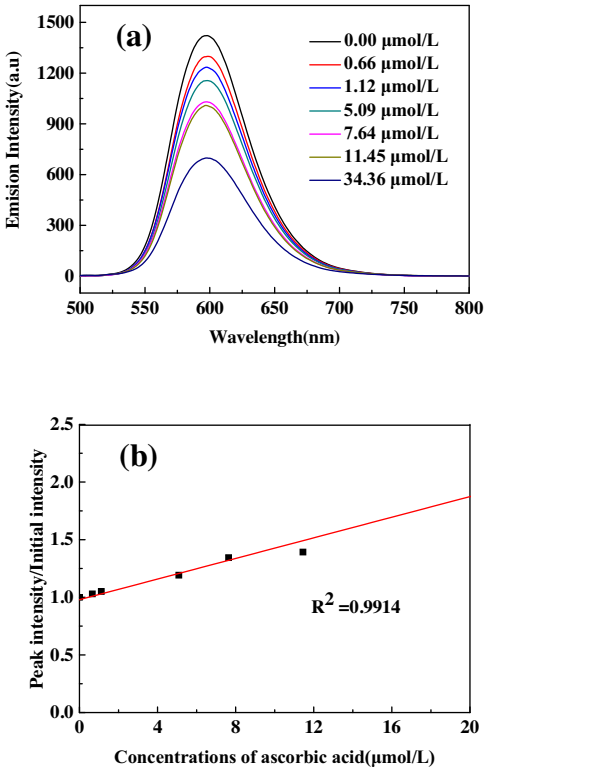

Fig. 5. Different concentrations of ascorbic acid quenching (a) and linear dependence of emission intensity versus different concentration of ascorbic acid in degassed acetonitrile: water (1:1) excited at 551 nm (top) and 600 nm (bottom) at room temperature; 0.02 mmol/L Ru complex (b).

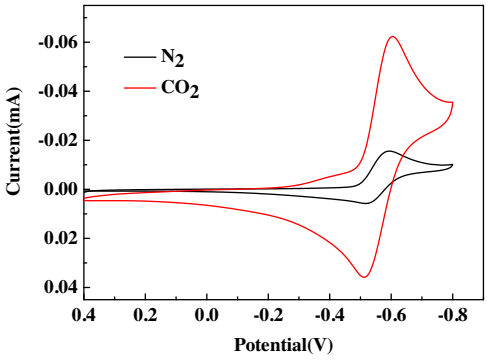

Fig. 6. The reduction pattern of pyridine under N_2 and CO_2 pressure with concentration of 10 mmol/L pyridine, 0.5 mol/L potassium chloride solution; scan rate, 5 mV/s; pH 5.

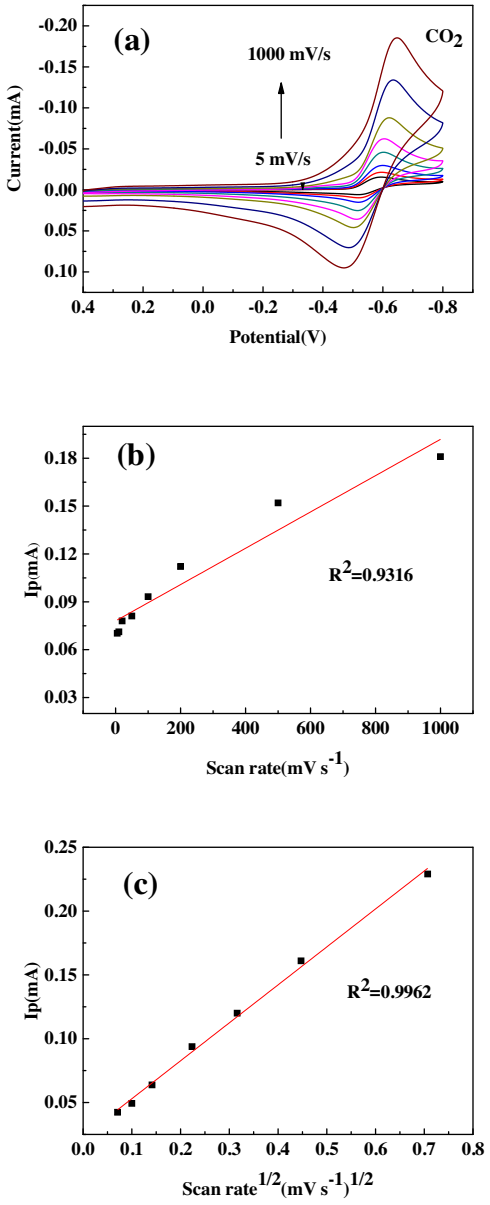

Fig. 7. CV of different scan rate (a) and linear dependence of peak current versus the scan rate (b) linear dependence of peak current versus the square root of the scan rate from 5 to 1000 mV/s (c).

same as the square root of the scanning rate following R^2, 0.9962. All the result indicated that the electrode was affected by adsorption and diffusion controlled [43,46–49]. This means that the reaction rate is not controlled by the number of active sites on the electrode surface, but rather the spread of CO_2 in the solution. At the reduction potential of pyridine, the reaction of CO_2 and pyridine was diffusion-limited controlled. Upon addition of CO_2, the diffusion limited current increased remarkably, while the potential shifted catholically, and the reversibility in the return oxidation wave was lost due to the chemical reaction between CO_2 and the electrocatalyst [43].

To study the effect of pH on the reduction current, the results are shown in Fig. 8.

Fig. 8 shows the effect of solution pH on the catalytic current density under CO_2 pressure. An irreversible reduction peak at approximately −0.6 V that increases with decreasing pH (hence increasing [PyH^+]). The large observable reductive feature at approximately −0.6 V was assigned to PyH^+ reduction to pyridine. The catalytic potentials decreased when the solution pH changed from 2 to 4 and kept stable during the pH of 4–5.3. After that, the catalytic potentials increased with the increase of solution pH. Therefore, the solution pH was set as 5 to keep the catalytic potential low [47].

In the process of photocatalysis, the electrolyte concentration plays an important role. Fig. 9 shows the effect of the concentration of pyridine on the reduction current. The difference of reduction peaks current between CO_2 and N_2 mapping with the concentration of pyridine are shown in Fig. 9(b).

As shown in Fig. 9(a), the intensity of reduction peak increased significantly with the increase of pyridine during the low pyridine concentration from 2.24 mmol/L to 5.24 mmol/L. In order to make it clear that effect of the concentration of pyridine, the difference of reduction peak currents under CO_2 and N_2 pressure mapping with

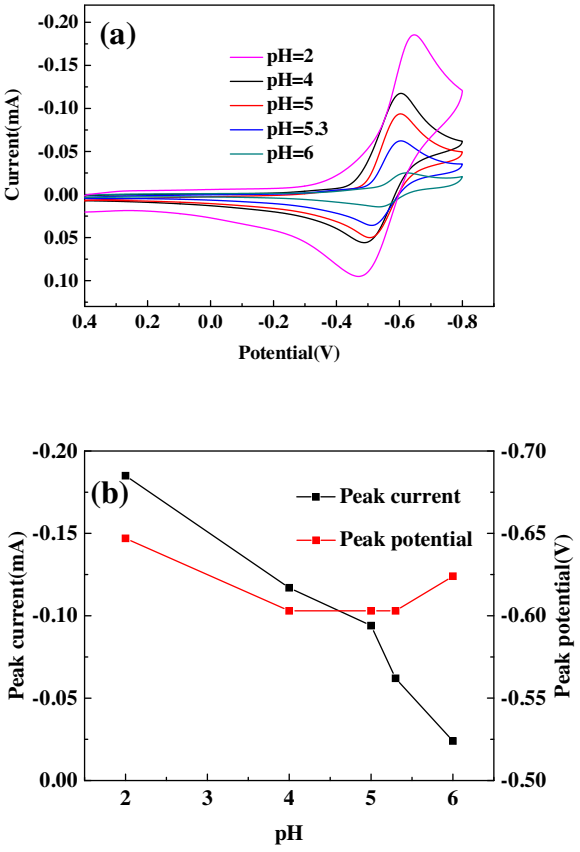

Fig. 8. CV under CO_2 with different pH (a) and linear of pH with peak current and potential (b).

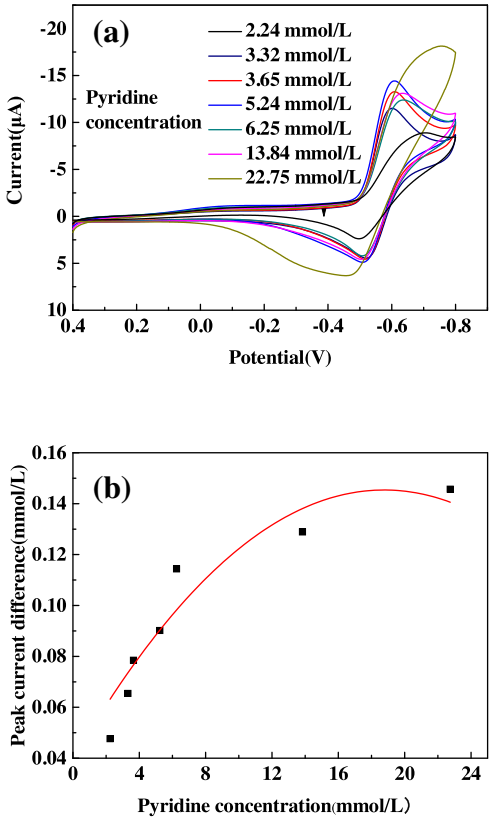

Fig. 9. CV and current difference with pyridine concentration diagram (a) and relation between peak currents deviation through N_2 and CO_2 and concentration of pyridine (b).

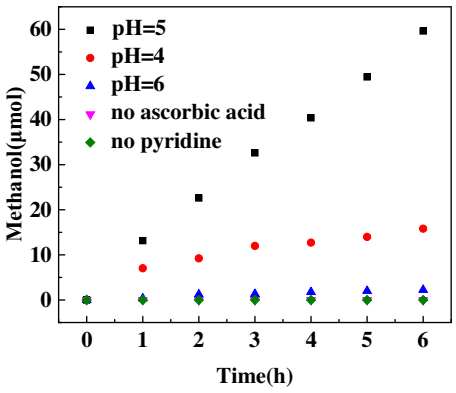

Fig. 10. Methanol concentration versus pH and reaction time.

the concentration of pyridine was studied and shown in Fig. 9(b). With the increase of pyridine concentration, the catalytic current difference increased till to a platform. It can be speculated that the redox reaction CO_2 may be limited by the high concentration of pyridine [50]. The photogenerated electron from the photosensitizer by the visible light irradiation should be transferred to a reaction center before the recombination of the photoinduced electron and holes. When the active sites on the surface of the catalyst matched the photoinduced electrons, the CO_2 reduction will perform smoothly. If the catalyst concentration was much high than photoinduced electrons could be generated by the photosensitizer, it would have a negative impact on the rate of electron transfer and catalytic effect. When pyridine concentration was higher than 6.35 mmol/L, there was another redox reaction which was not the conversion of CO_2 to methanol that need to be further studied. The experiment results showed that the best appropriate concentration of pyridine was 2–6 mmol/L which could be prepared with different conditions.

3.3. Experiment and reaction mechanism of photocatalytic system

The pH value of the solution was the most important factor for the catalytic current. Hence, in the photocatlytic reaction of the CO_2 conversion, the solution pH was chosen as an effect parameter for the product yield. The yield of methanol with different pH and time are shown in Fig. 10.

As shown in Fig. 10, with the increase of reaction time, the yield of methanol increased. And the system in pH 5 showed highest catalytic efficiency than that in pH 4 and 6. When the pH was 5 and the reaction time was 6 h, the yield of methanol reached 60 μmol/L. However, the yield of methanol was negligible when pH was 6, because H^+ was the vital to the process of photocatalycal reaction and a certain amount of H^+ can enhance the activity of catalyst [34]. The product methanol could not be determined when the ascorbic acid or pyridine were absent in the system.

Pyridine and Pyridinium ($pyrH^+$) were the species of interest in this work due to its proposed role in the CO_2 catalytic reduction. It could be inferred that at pH = 5, $pyrH^+$ participated in one of the several irreversible reactions: pyridinyl radical formation, dihydropyridine formation, and reduction of the weak acid protons to dihydrogen.

Although the CO_2 photoreduction mechanism is complex, it is well known that pyridine (Py) catalyzed the CO_2 reduction through the $PyCOOH^\bullet$ formation. There were consequential steps in this reaction. Protonated pyridine (PyH^+) could be reduced to pyridyl radical ($PyH^\bullet$) after getting an electron from one electron reduced photosensitizer. Then, the $PyH^\bullet$ species reacted with CO_2 to generate a $PyCOOH^\bullet$ through a proton transfer process. Finally, methanol

was formed from PyCOOH• through a series of proton-coupled electron transfer [42].

4. Conclusions

The photocatalytic reduction of CO_2 to methanol was performed in the present pyridine catalysis system under visible light irradiation. $[Ru(phen)_3](PF_6)_2$ was prepared as a photosensitizer and showed excellent visible light utilization activity and electron transfer properties. And in electrochemical experiments, pyridine showed clear catalytic reaction under CO_2 pressure compared that under N_2 pressure. The solution pH had important effect on the catalytic properties. By controlling variable methods for pyridine electrochemical tests, the optimize conditions of photocatalytic reduction of CO_2 was achieved: exposure to the light of 420 nm in the home-made light reaction; pH 5; 0.020 mmol/L of $[Ru(phen)_3](PF_6)_2$ as the chromophore; 5.24 mmol/L pyridine as catalyst degradation CO_2; 0.1 mol/L KCl and 0.2 mol/L ascorbic acid as a sacrificial reductant; the reaction time was 6 h, the concentration of the reduced product methanol at this time was 60 μmol/L, which proved that the selected ruthenium complexes had a valid photocatalytic reduction effect, and was qualified as the effective photocatalytic material.

Acknowledgements

This work was supported by the Beijing Higher Education Young Elite Teacher Project (No. YETP0773), the National Natural Science Foundation of China (No.51278053 and 21373032), and grant-in-aid from Kochi University of Technology.

References

[1] B.E. Conway, B.V. Tilak, Electrochim. Acta 47 (2002) 3571–3594.
[2] M. Gattrell, N. Gupta, A. Co, J. Electroanal. Chem. 594 (2006) 1–19.
[3] K.J.P. Schouten, E. Perez Gallent, M.T.M. Koper, J. Electroanal. Chem. 716 (2014) 53–57.
[4] H. Arakawa, M. Aresta, J.N. Armor, M.A. Barteau, E.J. Beckman, A.T. Bell, J.E. Bercaw, C. Creutz, E. Dinjus, D.A. Dixon, K. Domen, D.L. DuBois, J. Eckert, E. Fujita, D.H. Gibson, W.A. Goddard, D.W. Goodman, J. Keller, G.J. Kubas, H.H. Kung, J.E. Lyons, L.E. Manzer, T.J. Marks, K. Morokuma, K.M. Nicholas, R. Periana, L. Que, J. Rostrup-Nielson, W.M.H. Sachtler, L.D. Schmidt, A. Sen, G.A. Somorjai, P.C. Stair, B.R. Stults, W. Tumas, Chem. Rev. 101 (2001) 953–996.
[5] G.A. Olah, A. Goeppert, G.K.S. Prakash, J. Org. Chem. 74 (2009) 487–498.
[6] M. Mikkelsen, M. Jorgensen, F.C. Krebs, Energy Environ. Sci. 3 (2010) 43–81.
[7] M.S. Khan, M.N. Ashiq, M.F. Ehsan, T. He, S. Ijaz, Appl. Catal. A Gen. 487 (2014) 202–209.
[8] J. Li, D. Luo, C. Yang, S. He, S. Chen, J. Lin, L. Zhu, X. Li, J. Solid State Chem. 203 (2013) 154–159.
[9] X. Li, J. Wen, J. Low, Y. Fang, J. Yu, Sci. China Mater. 57 (2014) 70–100.
[10] B.S. Kwak, M. Kang, Appl. Surf. Sci. 337 (2015) 138–144.
[11] V. Viswanathan, H.A. Hansen, J.K. Nørskov, J. Phys. Chem. Lett. 6 (2015) 4224–4228.
[12] G. Centi, S. Perathoner, G. Wine, M. Gangeri, Green Chem. 9 (2007) 671–678.
[13] J. Schneider, H. Jia, J.T. Muckerman, E. Fujita, Chem. Soc. Rev. 41 (2012) 2036–2051.
[14] B. Kumar, M. Llorente, J. Froehlich, T. Dang, A. Sathrum, C.P. Kubiak, Annu. Rev. Phys. Chem. 63 (2012) 541–569.
[15] Y. Izumi, Coord. Chem. Rev. 257 (2013) 171–186.
[16] V.S. Thoi, N. Kornienko, C.G. Margarit, P. Yang, C.J. Chang, J. Am. Chem. Soc. 135 (2013) 14413–14424.
[17] J. Wen, X. Li, W. Liu, Y. Fang, J. Xie, Y. Xu, Chin. J. Catal. 36 (2015) 2049–2070.
[18] S. Ye, R. Wang, M.-Z. Wu, Y.-P. Yuan, Appl. Surf. Sci. 358 (2015) 15–27.
[19] L. Yuan, Y.-J. Xu, Appl. Surf. Sci. 342 (2015) 154–167.
[20] W. Zhang, F. Dong, W. Zhang, Appl. Surf. Sci. 358 (2015) 75–83.
[21] J. Low, B. Cheng, J. Yu, M. Jaroniec, Energy Storage Mater. 3 (2016) 24–35.
[22] C.D. Windle, R.N. Perutz, Chem. Rev. 256 (2012) 2562–2570.
[23] S. Kawamura, M.C. Puscasu, Y. Yoshida, Y. Izumi, G. Carja, Appl. Catal. A Gen. 504 (2015) 238–247.
[24] O. Ola, M.M. Maroto-Valer, Appl. Catal. A Gen. 502 (2015) 114–121.
[25] G. Ghadimkhani, N.R. de Tacconi, W. Chanmanee, C. Janaky, K. Rajeshwar, Chem. Commun. 49 (2013) 1297–1299.
[26] W. Lin, H. Frei, C.R. Chim. 9 (2006) 207–213.
[27] E.G. Ha, J.A. Chang, S. Byun, C. Pac, D.M. Jang, J. Park, S.O. Kang, Chem. Commun. 50 (2014) 4462–4464.
[28] Q. Zhou, Z. Fang, J. Li, M. Wang, Microporous Mesoporous Mater. 202 (2015) 22–35.
[29] S.N. Habisreutinger, L. Schmidt-Mende, J.K. Stolarczyk, Angew. Chem. Int. Ed. 52 (2013) 7372–7408.
[30] S. Das, W.M.A. Wan Daud, Renew. Sust. Energy Rev. 39 (2014) 765–805.
[31] G. Seshadri, C. Lin, A.B. Bocarsly, J. Electroanal. Chem. 372 (1994) 145–150.
[32] A.J. Morris, G.J. Meyer, E. Fujita, Acc. Chem. Res. 42 (2009) 1983–1994.
[33] M. Tahir, N.S. Amin, Energy Convers. Manag. 76 (2013) 194–214.
[34] A.M. Appel, J.E. Bercaw, A.B. Bocarsly, H. Dobbek, D.L. DuBois, M. Dupuis, J.G. Ferry, E. Fujita, R. Hille, P.J.A. Kenis, C.A. Kerfeld, R.H. Morris, C.H.F. Peden, A.R. Portis, S.W. Ragsdale, T.B. Rauchfuss, J.N.H. Reek, L.C. Seefeldt, R.K. Thauer, G.L. Waldrop, Chem. Rev. 113 (2013) 6621–6658.
[35] H. Hori, F.P.A. Johnson, K. Koike, O. Ishitani, T. Ibusuki, J. Photochem. Photobiol. A Chem. 96 (1996) 171–174.
[36] M. Kirch, J.M. Lehn, J.P. Sauvage, Helv. Chim. Acta 62 (1979) 1345–1384.
[37] T. Hirose, Y. Maeno, Y. Himeda, J. Mol. Catal. A Chem. 193 (2003) 27–32.
[38] B. Gholamkhass, H. Mametsuka, K. Koike, T. Tanabe, M. Furue, O. Ishitani, Inorg. Chem. 44 (2005) 2326–2336.
[39] Z.Y. Bian, K. Sumi, M. Furue, S. Sato, K. Koike, O. Ishitani, Inorg. Chem. 47 (2008) 10801–10803.
[40] Y. Tamaki, T. Morimoto, K. Koike, O. Ishitani, Proc. Natl. Acad. Sci. U. S. A. 109 (2012) 15673–15678.
[41] S. Sato, T. Morikawa, T. Kajino, O. Ishitani, Angew. Chem. Int. Ed. 52 (2013) 988–992.
[42] C.H. Lim, A.M. Holder, C.B. Musgrave, J. Am. Chem. Soc. 135 (2013) 142–154.
[43] Z.Y. Bian, H. Wang, W. Fu, L. Li, A.Z. Ding, Polyhedron 32 (2012) 78–85.
[44] M.N. Ackermann, L.V. Interrante, Inorg. Chem. 23 (1984) 3904–3911.
[45] Z.Y. Bian, K. Sumi, M. Furue, S. Sato, K. Koike, O. Ishitani, Dalton Trans. (2009) 983–993.
[46] A.J. Bard, L.R. Faulkner, Electrochemical Methods: Fundamentals and Applications, 2nd ed., Wiley, New York, 2001.
[47] A.J. Lucio, S.K. Shaw, J. Phys. Chem. C 119 (2015) 12523–12530.
[48] Q. Shi, H. Wang, S.L. Liu, L. Pang, Z.Y. Bian, Electrochim. Acta 178 (2015) 92–100.
[49] Q. Shi, H. Wang, S.L. Liu, Z.Y. Bian, RSC Adv. 4 (2014) 56263–56272.
[50] D.I. Won, J.S. Lee, J.M. Ji, W.J. Jung, H.J. Son, C. Pac, S.O. Kang, J. Am. Chem. Soc. 137 (2015) 13679–13690.